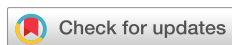


PAPERS | JANUARY 01 1995

Superconductivity: A guide to alternating current susceptibility measurements and alternating current susceptometer design

Martin Nikolo



Am. J. Phys. 63, 57–65 (1995)

<https://doi.org/10.1119/1.17770>



Articles You May Be Interested In

Combination high-sensitivity alternating current susceptometer and high-frequency B - H looper

Rev. Sci. Instrum. (August 1996)

In situ measurement of alternating current magnetic susceptibility of Pd–hydrogen system for determination of hydrogen concentration in bulk

Rev. Sci. Instrum. (July 2012)

Calibration of low-temperature ac susceptometers with a copper cylinder standard

Rev. Sci. Instrum. (February 2010)

Superconductivity: A guide to alternating current susceptibility measurements and alternating current susceptometer design

Martin Nikolo

Physics Department, St. Louis University, St. Louis, Missouri 63103

(Received 23 February; accepted 20 June 1994)

Since the arrival of high temperature superconductivity in 1987, the measurement of ac susceptibility has gradually become more popular as a large number of laboratories around the world have either already acquired an ac susceptometer or are in the process of doing so. Its advantage over other techniques is that it is an inductive, noncontact measurement that screens an entire volume of the sample. Here it is explained why this seemingly simple technique is very useful and the principle of measurement is explained in full detail. It is shown how to design and construct a low-cost susceptometer and how to interpret the data when applied to high temperature bulk superconductors. © 1995 American Association of Physics Teachers.

I. INTRODUCTION

Magnetic susceptibility is a measure of a sample's magnetization and it is defined as

$$\chi = M/H, \quad (1)$$

where M is the magnetization and H is the applied dc magnetic field. Similarly, ac susceptibility measurement involves an application of a varying magnetic field H_{ac} to a sample and recording the sample's response by a sensing coil. Here

$$\chi = \frac{dM}{dH_{ac}}. \quad (2)$$

In the dc measurement, the magnetic moment of the sample does not change with time. An ac output signal is detected but this signal arises from the periodic movement of the sample and therefore it does not represent the ac response of the sample itself. On the other hand, in an ac measurement the moment of the sample is changing in response to an applied ac field. Thus the dynamics of the magnetic system can be studied. This method also offers the opportunity to determine the frequency dependence of the complex susceptibility which leads to information about relaxation processes and the relaxation times of the magnetic systems studied.^{1,2}

This inductive method presents a rapid means of measuring samples without the need for current or voltage leads. ac susceptibility measurements have become popular with the advent of high temperature superconductivity. ac susceptibility can probe an entire sample volume and therefore it provides us with a volume average of the sample's magnetic response. This can be contrasted with resistivity measurements where the measuring current flows through a single, least resistance percolative path. Most frequently, ac susceptibility has been used to determine the onset temperature for diamagnetism at which a normal to superconducting transition takes place. This is the transition between a complete magnetic field shielding and the onset of magnetic flux penetration inside a superconducting sample.

The measurement of ac susceptibility can provide important information about the superconducting properties and ac losses in the polycrystalline high- T_c superconductors. In particular, the loss component or the imaginary part of the complex susceptibility can be used to probe the nature of the coupling between grains. In addition to the critical current density, the ac loss in the superconducting state is also an important parameter that determines the material's feasibility for use at low frequencies (<10 kHz). One can use ac sus-

ceptibility in the new granular oxides to find the transition temperatures of both the inter- and intragranular regions. One can use it to determine if separate phases are present and to find what fraction of a sample's volume is superconducting. In large dc magnetic fields a peak in the imaginary part of the susceptibility is defined as the onset of irreversibility.

II. PRINCIPLE OF MEASUREMENT

A. Theoretical outline

Let a varying ac field, $H_a = H_{a0} \cos \omega t$, be applied to a sample. In response to the ac field H_a , the local flux density B in the sample will show a phase lag behind the H field. For small applied ac fields the response will be nonlinear in the mixed state. This results in a distorted periodic wave form where neither B nor M can be expressed as a sinusoidal function of single frequency and the average local flux density $\langle B \rangle$ that threads the sample must be described by a Fourier expansion

$$\langle B \rangle = \mu_0 H_{a0} \sum_{n=1}^{\infty} [\mu'_n \cos(n\omega t) + \mu''_n \sin(n\omega t)]. \quad (3)$$

Here μ'_n and μ''_n are the real and imaginary parts of complex relative permeability μ_n . Now multiply both sides by $\cos(\omega t)$ and integrate over t from 0 to $2\pi/\omega$ (one period) to obtain

$$\int_0^{2\pi/\omega} \langle B \rangle \cos \omega t \, dt = \mu_0 H_{a0} (\pi/\omega) \mu'_1. \quad (4)$$

Similarly, multiply both sides of Eq. (3) by $\sin(\omega t)$ to get

$$\int_0^{2\pi/\omega} \langle B \rangle \sin \omega t \, dt = \mu_0 H_{a0} (\pi/\omega) \mu''_1. \quad (5)$$

However, the relative complex permeability, μ , is defined in terms of the complex, magnetic susceptibility, χ , as

$$\mu = 1 + \chi. \quad (6)$$

Therefore one can say

$$\chi'_1 = \mu'_1 - 1, \quad (7)$$

$$\chi''_1 = \mu''_1. \quad (8)$$

With the help of Eqs. (3)–(8) one can define the real, χ'_1 , and imaginary, χ''_1 , parts of susceptibility in terms of the local average magnetic induction $\langle B \rangle$ as

$$\chi'_1 = \left(\frac{\omega}{\pi \mu_0 H_{a0}} \int_0^{2\pi/\omega} \langle B \rangle \cos(\omega t) dt \right) - 1, \quad (9)$$

and

$$\chi''_1 = \left(\frac{\omega}{\pi \mu_0 H_{a0}} \int_0^{2\pi/\omega} \langle B \rangle \sin(\omega t) dt \right). \quad (10)$$

Therefore, one can see that χ'_1 gives us a quantitative expression for the amount of magnetic flux penetration into the sample. For a complete Meissner expulsion the integral in Eq. (9) vanishes and $\chi'_1 = -1$ and for a full flux penetration the integral is 1 and $\chi'_1 = 0$. Similarly for χ''_1 , in a completely superconducting state $\chi''_1 = 0$ while in the mixed superconducting state χ''_1 is a small (<1) positive number reflecting ac losses.

The principle of measuring ac susceptibility involves subjecting a sample to a small alternating magnetic field. The flux variation due to the sample is picked up by a sensing coil surrounding the sample and the resulting voltage induced in the coil is detected. This voltage is proportional to the time derivative of the sample's magnetization as will be shown here. Using the concept of mutual inductance one can derive an expression for χ in terms of directly measurable quantities.³ Here a long, cylindrical sample is assumed where the flux density distribution of a uniformly magnetized cylinder is the same as that of a solenoid of the same size so that the cylindrical sample can be modeled as an inner coil.

The total magnetic flux Φ sensed by the pickup coil may be calculated from either \mathbf{B} , the flux density, or the vector potential \mathbf{A} :

$$\Phi = \iint \mathbf{B} \cdot d\mathbf{a} = \int \mathbf{A} \cdot ds. \quad (11)$$

Here $d\mathbf{a}$ is the incremental area and ds is the incremental contour of the pickup coil, and thus the integration is over the entire pickup coil. A single pickup coil configuration is assumed for simplicity. The mutual inductance per solenoid primary turn is

$$L' = L_{sp}/N = \Phi/NI = (1/NI) \int \mathbf{A} \cdot ds. \quad (12)$$

L_{sp} is the mutual inductance between the solenoid primary coil and the pickup coil and I is the current in the primary coil. The emf induced in the pickup coil due to the primary coil is

$$v = -d\Phi/dt = -L_{sp}dI/dt. \quad (13)$$

But magnetization $M = NI/l$ where l is the length of the primary coil. Thus

$$v = -L'l dM/dt. \quad (14)$$

Now if one is dealing with the fundamental, $\chi = \chi_1$, only, and defines $M = \chi H$ together with the applied magnetic field $H = H_0 \cos 2\pi ft$, one gets

$$\chi = v_{rms}/(2\pi L'l f H_{rms}) \quad (15)$$

for the root mean square quantities v_{rms} and H_{rms} . Generally, we do not compute L_{sp} but rather experimentally determine a calibration constant α that reflects the coil geometry.

In an actual susceptometer two identical sensing coils are positioned symmetrically inside the primary coil and serve as the secondary coils in the measuring circuit (see Fig. 1.) The

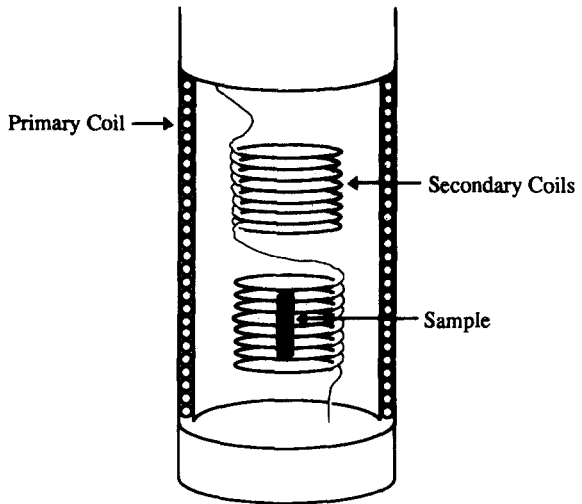


Fig. 1. Primary and secondary coil configuration.

two sensing coils are connected in opposition in order to cancel the voltages induced by the ac field itself or voltages induced by unwanted external sources. The sample is inserted in the lower coil. The measured rms voltage v across the two secondary coils wrapped tightly around the cylinder is

$$v(t) = -d\Phi/dt(mks). \quad (16)$$

With $M(t)$ denoting the magnetic induction inside the sample averaged over the volume V , the magnetic flux through the N turn oppositely wounded coils of radius a is

$$\Phi = \mu_0 \pi a^2 N M(t) \quad (17)$$

for $\Phi = \mu_0 \pi a^2 N [(M + H_a) - H_a]$. Therefore the measured voltage is

$$v(t) = -\mu_0 \pi a^2 N dM(t)/dt. \quad (18)$$

But for complex magnetic susceptibility χ'_n and χ''_n one can do a Fourier expansion of $M(t)$

$$M(t) = \sum_{n=1}^{\infty} H_{a0} (\chi'_n \cos n\omega t + \chi''_n \sin n\omega t). \quad (19)$$

Making use of Eq. (19), one obtains

$$v(t) = \mu_0 \pi a^2 \omega N H_{a0} \sum_{n=1}^{\infty} n (\chi'_n \sin n\omega t - \chi''_n \cos n\omega t). \quad (20)$$

Let $\mu_0 \pi a^2 \omega N H_{a0} = v_0$, then

$$v(t) = v_0 \sum_{n=1}^{\infty} n (\chi'_n \sin n\omega t - \chi''_n \cos n\omega t). \quad (21)$$

Here a lock-in amplifier can be set to measure the fundamental v_1

$$v_1 = v_0 (\chi'_1 \sin \omega t - \chi''_1 \cos \omega t). \quad (22)$$

This analysis predicts that higher harmonics of the χ' and χ'' signals should result from the hysteresis behavior of the flux moving in and out of the sample. Thus in their simplest

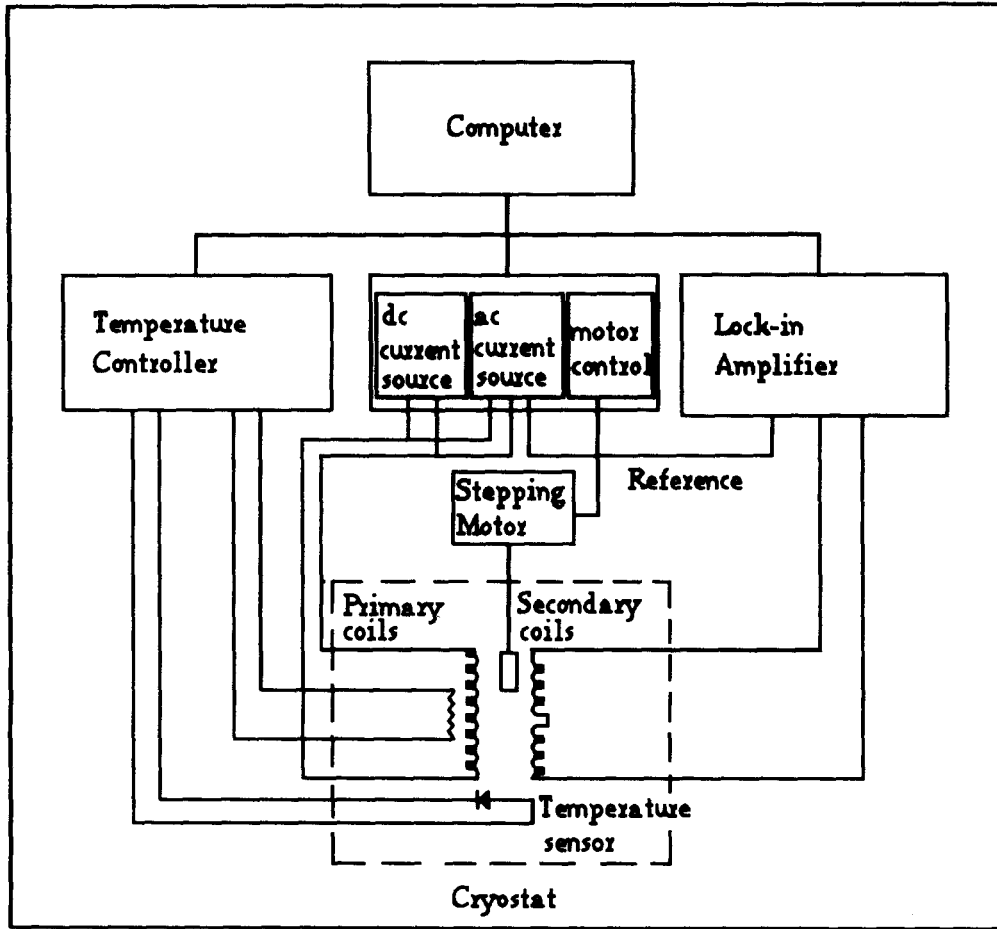


Fig. 2. Experimental arrangement of ac susceptibility apparatus.

form, the resulting χ'' signal would arise from a nonsinusoidal response in the ac susceptibility measuring coil. This nonlinear magnetic response arising in the granular high temperature superconductors can be confirmed by directly observing the wave forms induced in the secondary coils of the susceptometer on an oscilloscope.^{4,5} From here on the notation χ is used to denote the fundamental susceptibility which is the focus of this article.

Another way of examining the real and imaginary components of susceptibility is to point out that if loss elements exist in the sample, the induced voltage across the secondaries will involve a phase shift with respect to the voltage measured without the sample. This phase shifted signal can be decomposed into two components: one in phase with the voltage measured with no sample and the other in quadrature to it.

The magnetizing field H is measured in oersteds, which in free space is numerically equal to the flux density B that has units of gauss, i.e., 1 Oe = 1 G in vacuum. The unit of magnetic moment m is G cm³ (also called "emu"). The volume susceptibility $\chi = dM/dH$ formally has units of G/Oe and is dimensionless. In these units $\chi = -1/4\pi$ for an ideal, completely diamagnetic body in which the flux density $B = 0$ everywhere and similarly $\chi = -1$ in metric units for M and H both expressed in A/m.

Measuring the induced voltage with a lock-in amplifier, the real, χ' , and the imaginary, χ'' , parts of the susceptibility

can be separated. A classical ac susceptibility setup is shown in Fig. 2. Here an alternating magnetic field is generated by a solenoid that serves as the primary coil in a transformer circuit. The solenoid is driven with an ac current source with variable amplitude and frequency. A constant ac current source should be used if the temperature of the coil changes during the measurement. A dc field may also be applied by supplying a dc current to the primary coil. When a sample is placed within one of the sensing coils, the voltage balance is disturbed and the measured voltage, as shown in Eq. (15), is proportional to the amplitude of the fundamental of the ac susceptibility of the sample and several other parameters. Thus

$$v = (1/\alpha) V f H_a \chi, \quad (23)$$

where α is the calibration constant, V is the sample volume, and H_a and f are the magnitude and frequency of the applied magnetic field.

In designing the coil configuration, one can quite accurately calculate the voltage signal obtained, given the coil geometry, the applied field and frequency, and the sample volume. This can give one an advance idea of how carefully the coils will need to be balanced to sense the induced voltage due to the sample, and the system's sensitivity can be accurately estimated.

When the cylindrical samples are not too long, the measured χ should be corrected for demagnetization fields. This effect is a geometric one and accounts for the fact that the internal field in the sample may differ from the applied field. The true internal susceptibility is

$$\chi_{\text{int}} = \chi / (1 - D\chi), \quad (24)$$

where D is the demagnetization factor and χ is the measured or external susceptibility. χ_{int} is also sometimes called an absolute and χ a relative susceptibility.

It is impossible to make two identical sensing coils, and thus a slight offset voltage is read on the lock-in amplifier even when no sample is present. One can try to compensate for the imbalance by inventing a number of methods to improve the balance of the coils. Perhaps the most notable one is connecting a variable ratio transformer across the sensing coils. But even here, the balance point changes as either temperature, applied magnetic field, or frequency change making balancing a very difficult proposition indeed. One can avoid all these problems if one positions the sample in each coil and subtracts the signal to get the net sample voltage. For an offset voltage v_0 in one coil, one measures $v_1 = v + v_0$; in the second coil, $v_2 = -v + v_0$. Thus the true voltage can be determined by

$$v = (v_1 - v_2)/2. \quad (25)$$

The movement of the sample has to be controlled to high accuracy. This is accomplished with the help of a computer-controlled stepping motor. Here the top of the sample rod is attached to a nut that moves along a threaded shaft. This shaft is rotated by means of a stepping motor that can execute, for example, 1.8° steps. If the pitch of the thread is 3.5 mm, one step corresponds to 0.0175 mm.

B. Lock-in amplifier and phasing

The lock-in amplifier acts as a discriminating voltmeter. It measures the amplitude and the relative phase of an ac signal. Here, a reference signal having the same fundamental frequency as the desired measured signal and having a fixed phase relationship with it is provided. The lock-in amplifier acts as though it were a bandpass filter of enormously high Q with its center frequency at the desired signal frequency. The output of a lock-in amplifier is a magnified dc voltage proportional to its synchronous ac input signal. An excellent review on the operation of a lock-in amplifier was recently given in this journal by Scofield.⁶

Perhaps one of the most useful features of the ac susceptometer is that both the real or in-phase component χ' , and the imaginary or out-of-phase component, χ'' , can be measured. To measure both components, the lock-in detector requires a reference signal at the same frequency and in phase with the current from the ac current source.

χ'' must never be negative. A simple way to set the phase of the lock in is to put a known sample into a low-loss state. This can be done by taking, say, a $\text{YBa}_2\text{Cu}_3\text{O}_7$ pellet ($T_c = 90$ K) and subjecting it to a small field, i.e., 1.0 Oe or less, at low temperature, i.e., 40 K or less. In this regime χ'' should be zero. This will work reasonably well for most typical measurements. However, if precise frequency shifts are to be measured one needs to develop the following, more precise, procedure.

The reference signal tunes in the lock in and the lock-in amplifier provides an output E_{out} which is sensitive to the phase difference Φ between the input signal and reference signal E_{in}

$$E_{\text{out}} = E_{\text{in}} \cos \Phi. \quad (26)$$

By using the phase adjust Θ feature on the lock in, Φ can be determined using

$$E_{\text{out}} = E_{\text{in}} \cos(\Phi - \Theta). \quad (27)$$

When the lock-in output is at maximum $\Phi = \Theta$. In order to separate the real and imaginary components of χ , Θ must be determined. Once Θ is known, the lock-in amplifier signal measured at Θ will be proportional to χ' , and the signal measured at $\Theta + 90^\circ$ will be proportional to χ'' .

To maintain consistency in the data acquisition, all dual phase data are measured with the lock-in amplifier phase set to 0° and 90° . The phase angle Θ is then used to convert the measured voltages to the equivalent in-phase and out-of-phase voltage signal

$$V' = v_0 \cos \Theta + v_{90} \sin \Theta, \quad (28)$$

$$V'' = v_{90} \cos \Theta - v_0 \sin \Theta. \quad (29)$$

Here v_0 and v_{90} are the lock-in voltages at 0° and at 90° . V' is the in phase voltage (Θ), and V'' is the out-of-phase voltage ($\Theta + 90^\circ$).

If the temperature of the primary coil changes, the phase angle will vary with the changing resistance of the coil and the lock-in amplifier should be referenced to the voltage drop across a resistor, placed outside the cryostat, in series with the primary coil. On the secondary circuit, the input impedance of the lock-in amplifier is large enough to make any change in the coil resistance insignificant. The voltage signal across the secondary coils (inductive circuit) is to a first order 90° out of phase with the reference voltage signal, which in turn is in phase with voltage signal across a precision resistor in series with the driving primary coil.

III. ac SUSCEPTOMETER DESIGN

A. Primary and secondary coils

Before designing an ac susceptometer, one has to decide on the type of sample it will be used for and on the typical dimensions of the sample. The design will certainly differ depending on whether one wants to measure a bulk ceramic, a thin film, or a crystal.⁷ Also, one has to decide how large the ac fields are that one wants to obtain, and what is the maximum frequency of the desired field. Thus the design of the primary coil comes first. Using the long solenoid approximation one obtains for the magnetic field, B , inside the solenoid

$$B = \mu_0 N I / l. \quad (30)$$

Here μ_0 is the permeability of free space defined as $\mu_0 = 4\pi \times 10^{-7} \text{ N/A}^2$, N is the number of turns, l is the length of the solenoid, and I is the current.

The next step involves the apparatus available. That is, what is the maximum current one's current source together with the frequency generator can provide? Obviously, the answer will be partially linked to the total load, or total impedance of the primary coil driven. If we assume that we can neglect the capacitive coupling, the total impedance is

$$Z = \sqrt{R^2 + (\omega L)^2}. \quad (31)$$

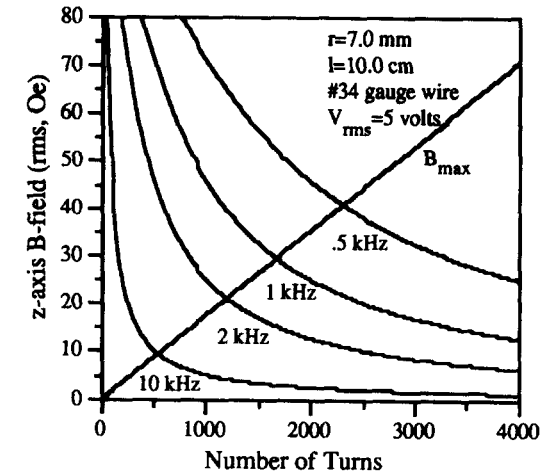


Fig. 3. Plot of axial magnetic field B inside a primary coil vs number of turns.

Here R is the resistance, and L is the self-inductance of the coil. Also, ω is the angular frequency of the driving ac field. The long coil approximation can be used to estimate the self-inductance L

$$L = \mu_0 N^2 A / l, \quad (32)$$

where A is the area of a single loop.

Examining Eqs. (30)–(32) more closely, it becomes obvious that in the attempt to increase the magnetic field, B , by increasing the number of turns, one also increases the self-inductance, L , by an even faster rate. This, in turn, reduces B by reducing the current in the coil. Therefore in the attempt to increase B , it is actually reduced. This consideration can be ignored for the design of a low field (10 Oe) susceptometer where the current source limitations are not serious. But for ac fields in the region of several hundred oersted, this becomes a formidable obstacle. One way of resolving this problem is to connect a power amplifier to the current source.

Knowing the maximum field desired, one gets an approximate idea of the maximum current needed, given the approximate dimensions of the coil. It seems advantageous to make the primary coil as short as possible. However, a short coil will not have a uniform axial field, which in turn means that even perfectly wound secondary coils will not see the same field and that will lead to voltage imbalance across the empty coils.

Figure 3 shows the result of calculation of maximum magnetic field allowed versus the number of turns for a fixed maximum ac current that can be provided by the current amplifier. This is the straight line. The series of curved lines gives a set of maximum fields that the coil allows us to send through it, given the finite voltage that the current amplifier can put across the coil and given the frequency dependent self-inductance of the coil. It is the point of intersection of the two calculated lines that will give us an optimal design given the finite limitations of the current amplifier. However, this optimal design is good only for a given frequency. At a lower frequency we still have the same maximum field since B_{\max} is still limited by the maximum current from the amplifier. For a higher frequency B_{\max} will drop, and it will be

determined by a new intersection of inductance dependent curve and the same linear current amplifier curve.

Designing the secondary sensing coils, one should strive for dimensions such that the sample volume is not negligible compared to that of the coil volume. This is because the pickup voltage is measured by comparing the flux displaced in one coil against the flux present in the empty, balancing coil. One should try to have the sample's volume as close as possible to the sensing coil volume. In the case of extremely tiny crystal samples, the volume of the crystals should occupy at least 5% of the volume of the coil or the measurement will not have the resolution to separate the crystal signal from the internal voltage offset. A larger number of turns on the secondaries will act as a voltage amplifier and will increase the sensitivity. Ideally, one wants to select the smallest wire diameter possible. For tiny single crystals the smallest possible coil is necessary. This dimension is limited by the size of the smallest temperature diode that will be inserted into the coil together with the sample holder. Also the coils should not be very close together to avoid flux coupling. A separation distance of about the length of a coil has been a reasonable and popular choice.

Although it is assumed that the two sensing coils are identical, in practice this never happens. One can have exactly the same number of turns on each coil such that the resistance is the same, but any slight imperfection in the windings will change the inductance and therefore the balance. Winding the coils with a very thin wire that one can barely see, remains an art form, especially if one tries to wind many layers without any imperfections.

The difficulty in balancing the coils is the reason why the optimal ac susceptibility design involves a stepping motor that moves the sampler holder into each coil and then subtracts the signal. In this way, any imbalance is subtracted. On the other hand, if one uses a simpler design in which the sample holder remains stationary in one of the coils, measuring absolute susceptibility is still possible but tedious. A small, variable, ratio transformer can be connected across the two secondary coils and used to improve the coil balance, but this balance holds only for a given field and frequency. Another method would be to use the nonuniform, decreasing field at the ends of the primary coil. By sliding the primary coil slightly along the two sensing coils, one can obtain a better balance. In conclusion, the single sample position coil design is useful if relative susceptibility is needed; otherwise, a moving sample holder design is preferable.

B. Calibration and sensitivity

One can find the calibration constant by calculating the mutual inductance, L_{sp} in Eq. (13), between the primary and sensing coils or the method of dipolar approximation can be used for the case of a small sample. When the dimension of the sample is small compared to the radius of the detection coil, R , the sample can be approximated by a magnetic dipole and then α , the calibration constant, defined in Eq. (23), can be determined by the geometry of the measuring coil^{8–10}

$$\alpha = \frac{10^8}{8\pi^2 n} \frac{(L^2 + d^2)^{1/2}}{L}, \quad (33)$$

where n is the number of turns/centimeter on the sensing coil, L is the length of the sensing coil in centimeters, and d is the diameter of the sensing coil in centimeters. The calibration constant α can be calculated exactly for arbitrary

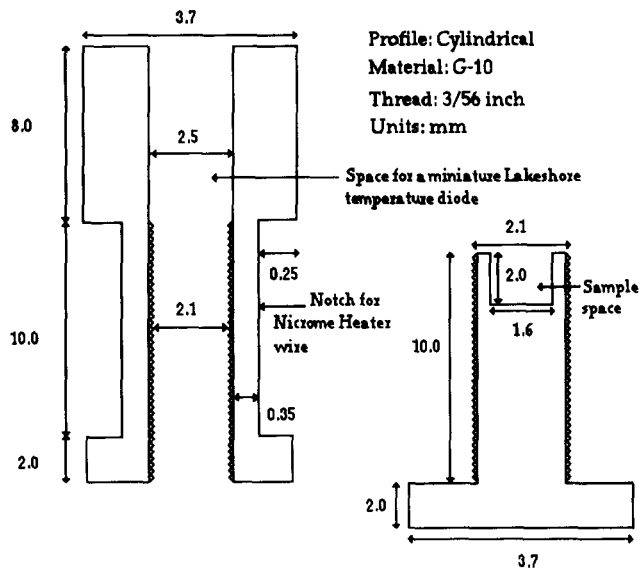


Fig. 4. Single crystal sample holder.

sample size by following the outline given in Eqs. (11)–(15). This has been done by Goldfarb and Minervini.³ The results show that for samples with dimensions comparable to the size of the sensing coil the calibration coefficient is valid to within 5%. The actual coefficient would be slightly larger.

Perhaps the more frequently used calibration is that with a known standard. However, here the resulting calibration is strictly valid only for the samples of the same size and shape

as the standard used. Al, Pt, Pd, and MnF₂ are popular standards. Precise value of α enables us to find the absolute magnetic volume susceptibility of the sample. One can further calculate the sensitivity of the apparatus. Magnetization M of a sample can be expressed in terms of its magnetic moment m and its volume V as $M = m/V$. Thus $\chi = m/(VH)$. But from Eq. (23) $\chi = \alpha v/(VfH)$, therefore $m = \alpha v/f$.

The above analysis was applied to the design of a high-field ac susceptometer for the measurement of single crystals. The average size of a single crystal is 1 mm, and therefore an extremely high sensitivity was desired. Figure 4 shows the dimensions of the sample holder. The dimensions were limited by the size (1.7 mm) of the smallest miniature temperature diode found (Lakeshore). Figure 5 shows the dimensions of the primary and secondary coils. The pickup coils in Fig. 5 are inserted into the primary coil and the sample holder in Fig. 4 is inserted into the lower pickup coil. The calibration constant, α was calculated using to be 1854. Assuming a voltage resolution of 10^{-7} V and the applied frequency of 1000 Hz gave a practical sensitivity of 1.85×10^{-7} emu.

C. Cryostat

Figures 6 and 7 show two cryostat designs. Figure 6 shows a very simple, low budget design for liquid nitrogen operation. This design was used for the single crystal susceptometer described above. The coil configuration was attached to quartz tubing and the entire body was then inserted to liquid nitrogen. A sample probe also made out of a narrow quartz tube was inserted in the cryostat. A heater close to the sample regulated the temperature between 77 K and above. A tiny

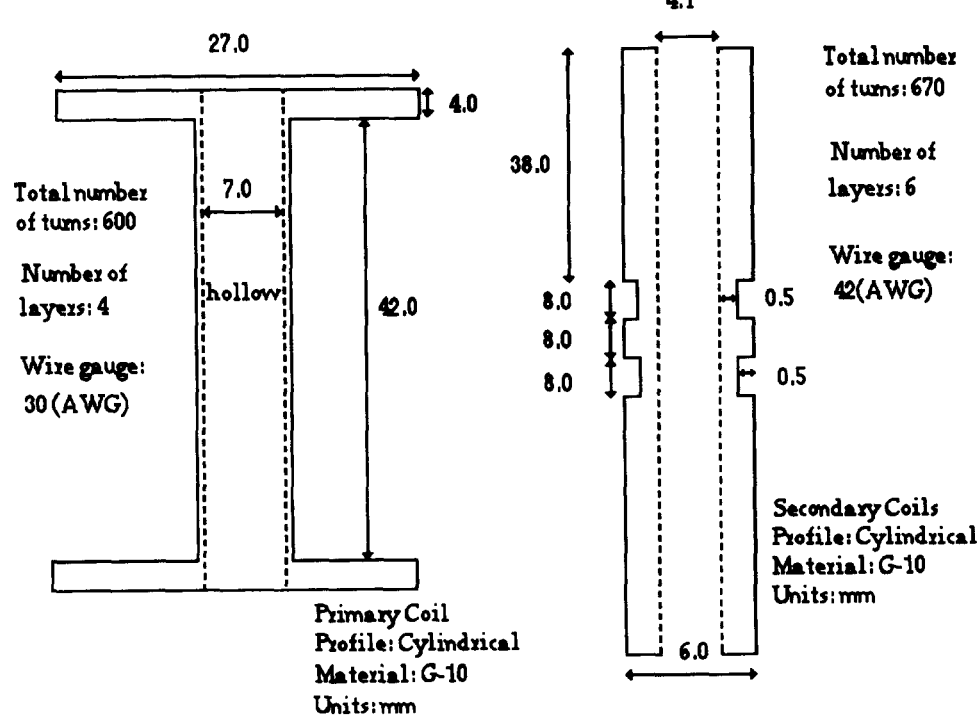


Fig. 5. Primary and secondary coil geometry.

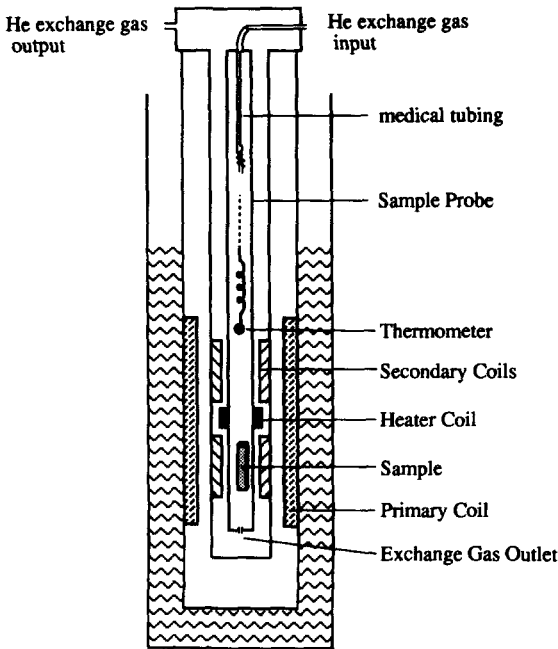


Fig. 6. Low budget cryostat.

plastic medical tubing run through the hollow section of the sample probe toward the sample space to provide helium exchange gas flow through the sample space. Its function was to provide a more uniform temperature environment.

Figure 7 shows a more advanced design that involves a vacuum jacket around the sample space. The coil probe is also inserted into the liquid cryogen. But here the tip of the

probe has a heater and a capillary such that some of the cryogen is sucked in by pumping on the sample space and vaporized before it reaches the sample. Here it is critical that the sample space is well thermally insulated from the cryogen bath. Otherwise the temperature control becomes quite difficult. That is, if the outer vacuum jacket has a leak this will not work. Also, this configuration will work better for liquid helium operation because its latent heat of vaporization is very small, 20.9 J/g. Liquid nitrogen's heat of vaporization is 198 J/g and here one has to put in a heat exchanger (for instance, a copper block) to be more effective in vaporizing the nitrogen. There are a number of other possible cryostat configurations that the reader should review before finalizing one's cryostat design.¹¹⁻¹³

D. Materials selection

One has to be very careful in selection of the materials in the vicinity of the sample space. The chosen materials should be (i) nonmagnetic, (ii) poor electrical conductors, and (iii) good thermal conductors. At the same time they should have minimal thermal expansion properties. These criteria narrow the range of plausible materials considerably. If financial issues are not a factor then sapphire (Al_2O_3) would be the best choice. However, most of us operate on limited budgets and the next best alternative must be found. That choice would be a plastic. Here we need a plastic that is not too soft and also one that undergoes a minimal thermal expansion. G-10, a greenish looking plastic also known as phenolic, has been the choice of many cryogenic workers. A less sturdy choice but perhaps easier to work with is glass. But here one needs to keep in mind that Pyrex does have a nonsignificant magnetic moment. Quartz in that respect is better but at the same time more fragile.

In more sophisticated systems where an outside jacket (concentric tubing) around the coil configuration is made and which is kept evacuated to improve temperature control, metallic casing is necessary to avoid horrendous vacuum leak problems that can easily occur if the jacket is made out of plastics. Here the best choice for the metal would be stainless steel. However, one has to be careful here. The most popular stainless steel is 304 and this steel can easily become ferromagnetic upon thermal cycling because it undergoes a martensitic phase transformation. The best choice is 310 and possibly 316. To further minimize any eddy current problems the thickness of the tubing should be as small as possible. Copper should be avoided at all costs!

IV. APPLICATION OF ac SUSCEPTIBILITY TO HIGH TEMPERATURE SUPERCONDUCTORS

The susceptibility transition in polycrystalline samples shows two steps: the first is due to the transition within grains and the second is due to the occurrence of the superconducting coupling between grains. An inflection point in the real part of the susceptibility curve separates the two transitions. This is due to the considerable difference between the lower critical magnetic field of the intergranular matrix and that of the grains. The lower critical field of the intergranular matrix is much smaller than that of the grains. Therefore, the flux penetrates the intergranular matrix first before it starts penetrating the grains. In the imaginary part (χ''), one observes two peaks that reflect energy dissipation (see Fig. 8).^{1,2}

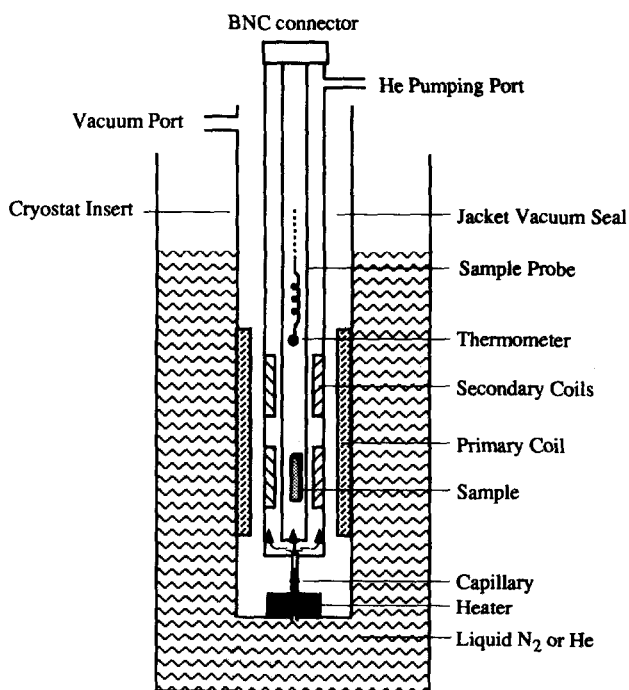


Fig. 7. Cryostat incorporating a vacuum jacket.

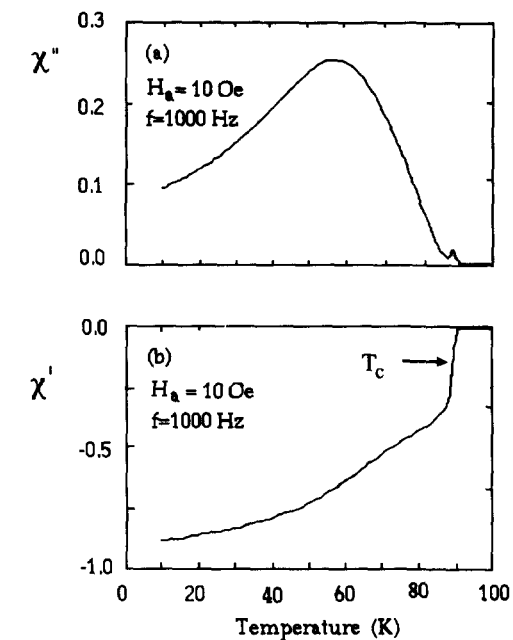


Fig. 8. Real (χ') and imaginary (χ'') parts of susceptibility vs temperature at 10 Oe and 1000 Hz.

As temperature increases toward T_c from below, flux lines and bulk shielding currents penetrate the material in a magnetic field of 800 A/m (10 Oe) at 1000 Hz. Shown are (a) the coupling and intrinsic peaks in χ'' (the intrinsic peak considerably smaller in size), and (b) the intrinsic (steep) and coupling components of χ' measuring field exceeds the lower critical field. This creates losses that are primarily hysteretic in character. When the flux lines and shielding currents fully penetrate the material, the losses reach a maximum. As the temperature increases beyond T_c , the shielding currents recede and the losses drop to zero. These same processes occur around T_c of the grains (intrinsic) or of the grain boundaries (coupling) (see Fig. 9). The shielding currents penetrate toward the center of the sample. At that time the losses are maximum. As the field increases further, the shielding currents and the ac losses decrease.

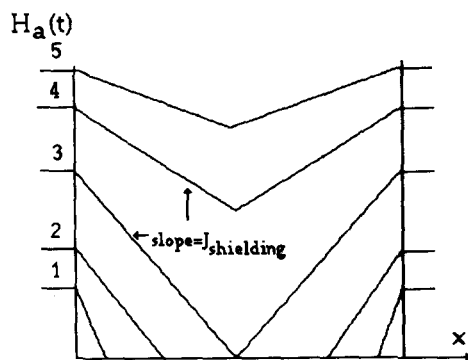


Fig. 9. Schematic flux profile inside a slab for a time varying external magnetic field. Here x represents position across the sample.

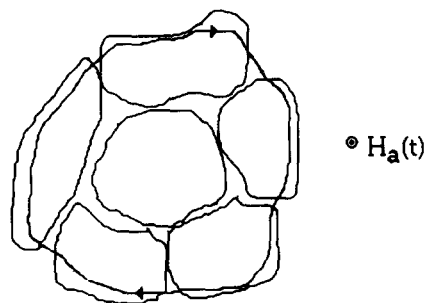


Fig. 10. Induced shielding current loop along the surface of a granular sample. The applied magnetic field $H_a(t)$ points into the page.

Far below T_c when the grains are coupled, the induced current from the external ac magnetic field results in shielding currents along the sample's outermost surface. In a real ceramic sample, the junctions are connected in a complicated series and parallel arrangement; however, in the presence of a small magnetic field, a network of superconducting junctions can be approximated by a single superconducting loop with a single junction (see Fig. 10).

The coupling peak is distinct for fields as low as 0.8 A/m (0.01 Oe). At that field, the peak is positioned in a temperature at about the intrinsic T_c of the grains. As the field amplitude is increased, the peak is shifted to lower temperatures and broadens (see Fig. 11). For temperatures above the peak temperature, for a given measuring field, the grains are decoupled. Below the peak, the grains are coupled, which permits the real part (χ') of susceptibility to reach -1 (SI) in small fields. For a field of 1.6 kA/m (20 Oe), χ'' peaks at 4 K. This field is called the measured decoupling field for this sample (see Fig. 12).

The intrinsic peak, shown in Figs. 12 and 8(a), is barely visible until the applied field reaches about 800 A/m (10 Oe). Its height is several times smaller than that of the coupling peak. Its position shifts very little in temperature as the field is increased from 0.8 A/m (0.01 Oe) to 4.8 kA/m (60 Oe).

The real part of susceptibility (χ') shows a drop from 0 to as low as -1, depending on temperature and the field ampli-

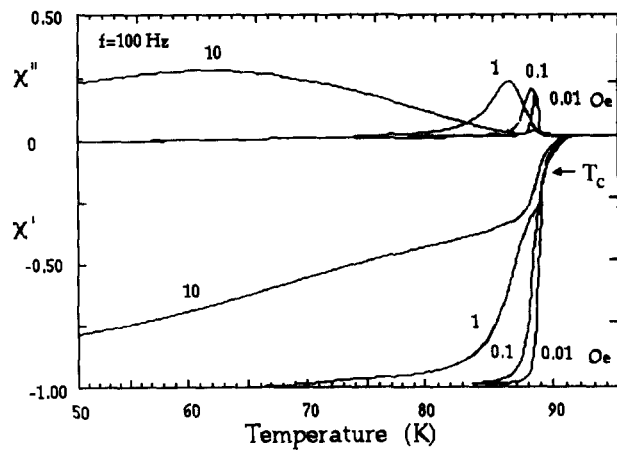


Fig. 11. Real (χ') and imaginary (χ'') parts of susceptibility for various applied magnetic fields for frequency of 100 Hz.

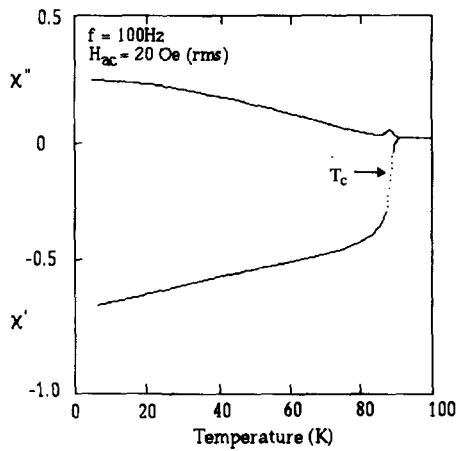


Fig. 12. Real (χ') and imaginary (χ'') parts of susceptibility for an applied field of 20 Oe. The broad peak is intergranular while the small peak is intrinsic.

tude [Fig. 8(b)]. The drop has an inflection point. The intrinsic component corresponds to the steep drop at 90 K. The coupling component is the second segment that decreases less steeply in temperature. It is particularly distinct at fields of 80 A/m (1 Oe) and above.

The intrinsic component of χ' is nearly insensitive to the applied magnetic field. There is no shift in temperature as the field increases from 0.8 A/m (0.01) to 1.6 kA/m (20 Oe). The coupling component, on the other hand, significantly shifts to lower temperature as the field is increased in this range. This can be easily understood in terms of the lower critical field. The intergranular matrix has a lower critical field which is several orders of magnitude smaller than that of the grains. Therefore in the low fields of measurement there will be very little to no flux penetrating the grains and thus there will be virtually no flux creep inside the grains. The relative sizes of the inter- and intragranular peaks, which reflect hysteretic losses due to flux creep, in Figs. 8(a) and 12, confirm this explanation.

V. SUMMARY

In this work the principle of ac susceptibility is explained and the measurement is described in detail. Design guidelines such as the geometry of the coils, cryostat, and materials selection are established. Calibration and the sensitivity of the instrument are explained. And finally, it is shown how an ac susceptometer can be effectively applied to the measurement of high temperature superconductors. The author hopes that this proves to be a starting guide for people interested in pursuing ac susceptibility measurements.

¹M. Nikolo, "Measurement of Flux Creep in High Temperature Superconductors by ac Susceptibility," Ph.D. thesis, University of Colorado, Boulder, 1991.

²M. Nikolo and R. B. Godfarb, "Flux creep and activation energies at the grain boundaries of Y-Ba-Cu-O superconductors," *Phys. Rev. B* **39**, 6615–6618 (1989).

³R. B. Goldfarb and J. V. Minervini, "Calibration of ac susceptometer for cylindrical specimens," *Rev. Sci. Instrum.* **55**, 761–764 (1984).

⁴K.-H. Müller, J. C. MacFarlane, and R. Driver, "Josephson vortices and flux penetration in high temperature superconductors," *Physica C* **158**, 69–75 (1989).

⁵W. Win, L. E. Wenger, J. T. Chen, E. M. Logothetis, and R. E. Solitis, "Nonlinear magnetic response of the complex ac susceptibility in the $\text{YBa}_2\text{Cu}_3\text{O}_7$ superconductors," *Physica C* **172**, 233–241 (1990).

⁶J. H. Scofield, "Frequency-domain description of a lock-in amplifier," *Am. J. Phys.* **62**, 129–133 (1994).

⁷Samples can be purchased from Colorado Superconductor, P.O. Box 8223, Fort Collins, CO 80526, Fax: (303) 490-1301. Upon request, any national laboratory such as Argonne will be happy to provide one.

⁸W. R. Abel, A. C. Anderson, and J. C. Wheatley, "Temperature measurements using small quantities of cerium magnesium nitrate," *Rev. Sci. Instrum.* **35**, 444–448 (1964).

⁹M. Couach, A. F. Khoder, and F. Monier, "Study of superconductors by a.c. susceptibility," *Cryogenics* **25**, 695–699 (1985).

¹⁰A. F. Khoder and M. Couach, "Calibration constant calculations for magnetic susceptibility measurements," *Cryogenics* **31**, 763–767 (1991).

¹¹G. K. White, *Experimental Techniques in Low-Temperature Physics*, 3rd ed. (Clarendon, Oxford, 1979), pp. 171–200.

¹²J. R. Owers-Bradley, Wen-Sheng Zhou, and W. P. Halperin, "Simple wide temperature range ac susceptometer," *Rev. Sci. Instrum.* **52**, 1106–1108 (1981).

¹³A. Edgar and J. W. Quilty, "A mutual inductance apparatus for measuring magnetic susceptibility and electrical conductivity," *Am. J. Phys.* **61**, 943–946 (1993).

FRANCIS BACON ON THE PURPOSE OF SCIENCE

As to the purpose of science, Bacon's name is so closely associated with the notion that its purpose is to secure power over nature ("human knowledge and power meet in one") that we forget that there are many more typical passages in Bacon in which he advocated a much more humbly meliorist position.

One can defend the view, which is also my own, that Bacon believed that the purpose of science is to make the world a better place to live in. In his preface to *The Great Instauration* (the compendious title of Bacon's entire system of philosophy), he wrote: "I would advise all in general that they would take into serious consideration the true and genuine ends of knowledge; that they seek it neither for pleasure, or contention, or contempt of others or for profit or fame, or for honour and promotion; or suchlike adulterate or inferior ends: but for the merit and emolument of life, and that they regulate and perfect the same in charity: for the desire of power was the fall of angels; the desire of knowledge the fall of man; but in charity there is no excess, neither men nor angels ever incurred danger by it."

Peter Medawar, *The Limits of Science* (1984). (Reprinted by Oxford University Press, New York, 1987), pp. 39–40.